Biomechanical Design of the Berkeley Lower Extremity Exoskeleton (BLEEX)

Adam B. Zoss, H. Kazerooni, *Member, IEEE*, and Andrew Chu

Abstract—Wheeled vehicles are often incapable of transporting heavy materials over rough terrain or up staircases. Lower extremity exoskeletons supplement human intelligence with the strength and endurance of a pair of wearable robotic legs that support a payload. This paper summarizes the design and analysis of the Berkeley lower extremity exoskeleton (BLEEX). The anthropomorphically based BLEEX has 7 DOF per leg, four of which are powered by linear hydraulic actuators. The selection of the DOF, critical hardware design aspects, and initial performance measurements of BLEEX are discussed.

Index Terms—Biomimetics, exoskeletons, mechatronics, robotics.

I. INTRODUCTION

HEAVY objects are typically transported by wheeled vehicles. However, many environments, such as rocky slopes and staircases, pose significant challenges to wheeled vehicles. Within these settings, legged locomotion becomes an attractive method of transportation since legs can adapt to a wide range of extreme terrains. Berkeley's lower extremity exoskeleton (BLEEX) is the first field-operational robotic system that can be worn by its operator and provides the ability to carry significant loads with minimal effort over any type of terrain. This is accomplished through four critical features: a novel control scheme, high-powered compact power supplies, special communication protocol and electronics, and a design architecture to decrease the complexity and power consumption. This paper focuses on the design architecture.

BLEEX comprises two powered anthropomorphic legs, a power supply and a backpack-like frame on which a variety of heavy payloads can be mounted (Fig. 1). BLEEX provides load-carrying capability through legged locomotion guided by human interaction; but instead of actively "driving" the vehicle, BLEEX shadows the operator's movement as he/she "wears" it like a pair of artificial legs. By combining the strength capabilities of robotics with the navigational intelligence and adaptability of humans, BLEEX allows heavy loads to be carried over rough, unstructured, and uncertain terrains. Possible applications include helping soldiers, disaster relief workers, wildfire fighters, and other emergency personnel to carry major loads without the strain typically associated with demanding labor.

A. B. Zoss and H. Kazerooni are with the Mechanical Engineering Department, University of California, Berkeley, CA 94720 USA (e-mail: azoss@me.berkeley.edu; exo@berkeley.edu).

A. Chu is with Siemens, Concord, CA 94520 USA (e-mail: archmage.chu@gmail.com).
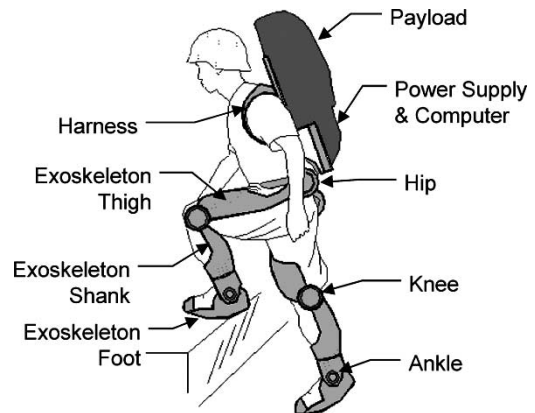
Fig. 1. Conceptual sketch of a lower extremity exoskeleton. Proper actuation of the robotic legs removes the payload weight from the wearer, while allowing the wearer to effortlessly control and balance the machine.

II. BACKGROUND

In the late 1960s, the first active exoskeletons were developed almost simultaneously at General Electric (GE) [1] and the Mihajlo Pupin Institute in Belgrade [2]. Safety concerns and complexity prevented the Hardiman project at GE from walking and the Belgrade exoskeleton followed only preprogrammed walking motions. Both projects were tethered to a stationary power source.

More recently, a lightweight power assist device, HAL, has been developed at the Tsukuba University [3]. Although the device successfully walks and carries its own power supply, it is designed to only assist the wearer's muscles; it cannot carry an external load. The Kanagawa Institute of Technology has developed a full-body "wearable power suit," powered by unique pneumatic actuators [4]. It has been demonstrated in limited applications without a portable power supply.

Still in development are several other lower extremity exoskeletons designed to aid disabled people [5]–[7]. Similar to exoskeletons, a variety of powered orthoses are being developed for the knee [8], [9], lower back [10], and ankle [11].

The BLEEX project is an energetically autonomous exoskeleton capable of carrying its own weight plus an external payload. All previous exoskeletons are either tethered to a fixed power supply or not strong enough to carry an external load. Unlike orthoses and braces, BLEEX transfers the payload forces to the ground, instead of the wearer.

III. EXOSKELETON CONTROL

The BLEEX control algorithm ensures that the exoskeleton shadows the operator with minimal interaction forces between

TABLE I
BLEEX ELECTRONICS REQUIREMENTS

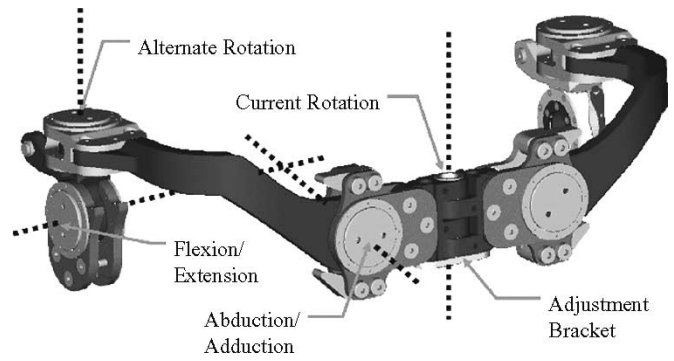| Electronics	Qty. per actuator	Qty. per exoskeleton
Encoder	1	8
Linear accelerometer	2	16
Single axis force sensor	1	8
Servo valve	1	8
RIOMs	1	10
Foot switches	N/A	2
Load distribution sensor	N/A	2
Inclinometer	N/A	1
Control computer	N/A	1

Fig. 2. BLEEX hip DOF (back view). Only the rotation axis does not pass through the human hip ball and socket joint. The adjustment bracket is replaceable to accommodate various sized operators.
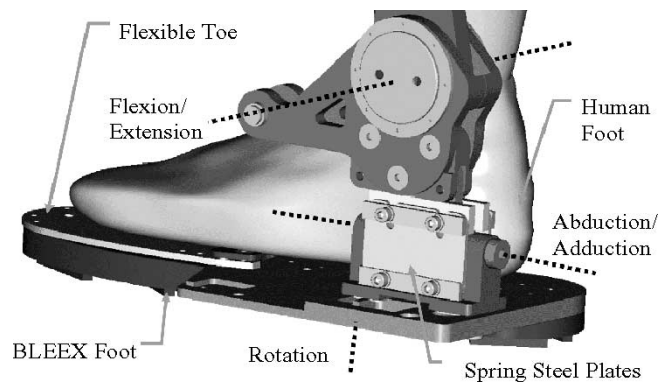

Fig. 3. BLEEX ankle DOF. Only the flexion/extension axis passes through the human's ankle joint. Abduction/adduction and rotation axes are not powered, but are equipped with appropriate impedances.

the two. The highlight of the control scheme is that it is solely based on measurements from the exoskeleton; there are no direct measurements from the operator or from where the operator contacts the exoskeleton (e.g., no force sensors between the two) [12]. This eliminates the problems associated with measuring interaction forces or human muscle activity.

Through the control algorithm, BLEEX instantaneously shadows the wearer's voluntary and involuntary movements. This requires the controller to be very sensitive to all forces and torques the operator imposes on the exoskeleton. To achieve this, the BLEEX control increases the closed loop system sensitivity to the operator's forces and torques [12].

The BLEEX control scheme uses a full dynamic model of the exoskeleton and utilizes a significant number of sensors to solve the dynamic model and control its actuators; thus, BLEEX contains a large amount of electronics. Each actuated joint contains an encoder and a pair of linear accelerometers to determine the joint's angle, angular velocity, and angular acceleration. An inclinometer gives the overall orientation relative to gravity. Servo valves and single-axis force sensors provide control and feedback of the actuation forces. Foot switches determine when the exoskeleton feet touch the ground and load distribution sensors determine how the operator distributes their own weight between their two feet in double stance. All the sensors connect to a distributed network of electronic boards (remote I/O modules or RIOMs), which then connect to a centralized controlling computer [13]. Table I summarizes the amount of electronics required for the BLEEX control algorithm.

IV. DEGREES OF FREEDOM

To ensure maximum safety and minimum collisions with the environment and operator, the BLEEX architecture is almost anthropomorphic. This means the BLEEX leg is kinematically similar to a human's, but does not include all of the degrees of freedom (DOF) of human legs. Additionally, the BLEEX degrees of freedom are all purely rotary joints. While the details of these joints differ from human joints, BLEEX has hip, knee, and ankle joints, like in a person. Overall, BLEEX has seven distinct DOF per leg:
a) 3 DOF at the hip;
b) 1 DOF at the knee (pure rotation in the sagittal plane);
c) 3 DOF at the ankle.
It is natural to design a 3-DOF exoskeleton hip joint such that all three axes of rotation pass through the human ball and socket hip joint. However, going through the design of several

mock-ups and experiments we learned that these designs have limited ranges of motion and result in singularities at some human hip postures. Therefore, the rotation joint was moved so that it does not align with the human's hip joint. Initially the rotation joint was placed directly above each exoskeleton leg (labeled "alternate rotation" in Fig. 2). This worked well for the lightweight plastic mock-up, but created problems in the full-scale prototype because the high mass of the torso and payload created a large moment about the unactuated rotation joint. Therefore, the current hip rotation joint for both legs was chosen to be a single axis of rotation directly behind the person and under the torso (labeled "current rotation" in Fig. 2). The current rotation joint is typically a spring loaded toward its illustrated position using sheets of spring steel.

Similar to the human's ankle, the BLEEX ankle also has 3 DOF. The flexion/extension axis coincides with the human ankle joint. For design simplification, the abduction/adduction and rotation axes on the BLEEX ankle do not pass through the human's leg and form a plane outside of the human's foot (Fig. 3). To take load off of the human's ankle, the BLEEX ankle abduction/adduction joint is sprung toward vertical, but the rotation joint is completely free.

Additionally, the front of the exoskeleton foot, under the operator's toes, is compliant to allow the exoskeleton foot to flex with the human's foot (see Section IX-A). Since the human and
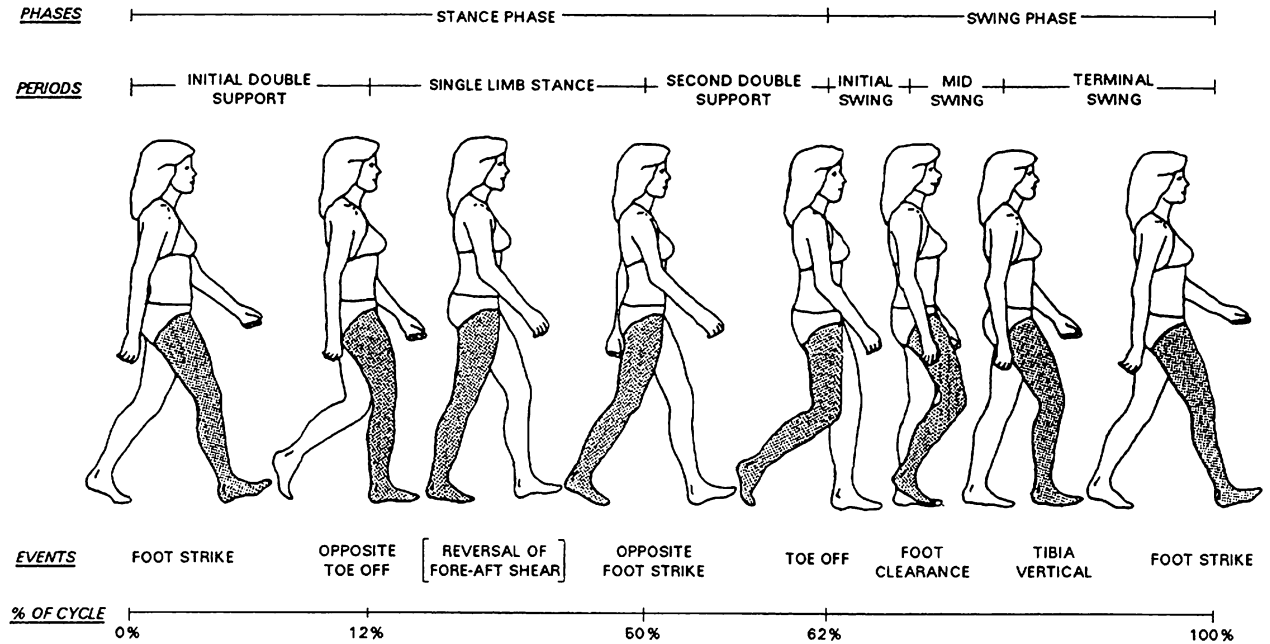
Fig. 4.   Human walking cycle [18]. The walking cycle begins with the start of stance phase (foot on the ground) at heel strike followed by toe-off and swing phase (foot off the ground) beginning at ∼60% of the cycle.

exoskeleton leg kinematics are not exactly the same (merely similar), the human and exoskeleton are only rigidly connected at the extremities (feet and torso).

V. CLINICAL GAIT ANALYSIS (CGA) DATA

A. Design by Biological Analogy

Each BLEEX leg has 7 DOF (besides the toe flexibility), but actuating all of them creates unnecessarily high-power consumption and control complexity. Instead, only joints that require substantial power should be actuated. Since we intended to design an anthropomorphic exoskeleton with limb masses and inertias same as in a human, the required joint torques and power for the exoskeleton to perform a given motion were approximated as that required by a similarly sized human performing the same motion. Additionally, since the primary goal of a lower-extremity exoskeleton is locomotion, the joint power requirements for the BLEEX were determined by analyzing the walking cycle shown in Fig. 4.

Human joint angles and torques for a typical walking cycle were obtained in the form of independently collected CGA data. CGA angle data is typically collected via human video motion capture. CGA torque data is calculated by estimating limb masses and inertias and applying dynamic equations to the motion data. Given the variations in individual gait and measuring methods, three independent sources of CGA data [14]–[16] were utilized for the analysis and design of the BLEEX. This data was further modified to yield estimates of exoskeleton actuation requirements. The modifications included 1) scaling the joint torques to a 75-kg person (the projected weight of the BLEEX and its payload not including its wearer) and 2) summing the pelvic tilt angle (or lower back angle depending on
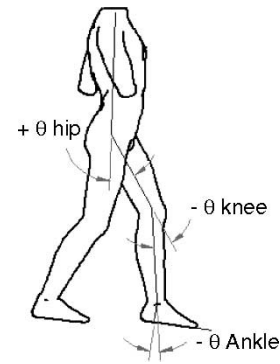

Fig. 5.   Angle and torque sign conventions. Each joint angle is measured as the positive counterclockwise displacement of the distal link from the proximal link (zero in the standing position).

data available) and the hip angle to yield a single angle between the torso and the thigh as shown in Fig. 5. This accounted for the reduced DOF of the exoskeleton. The following sections describe the use of CGA data for exoskeleton design. The sign conventions used are shown in Fig. 5.

B. Ankle

Fig. 6 shows the CGA ankle angle data for a 75-kg human walking on flat ground at approximately 1.3 m/s vs. time. As can be seen in all the plots, heel strike occurs at ∼0% of the step cycle and toe-off occurs at ∼60% of the step cycle.

Fig. 7 shows the adjusted CGA data of the ankle flexion/extension torque. The ankle torque is almost entirely negative, making unidirectional actuators an ideal actuation choice. This asymmetry also implies a preferred mounting orientation for asymmetric actuators (one-sided hydraulic cylinders).
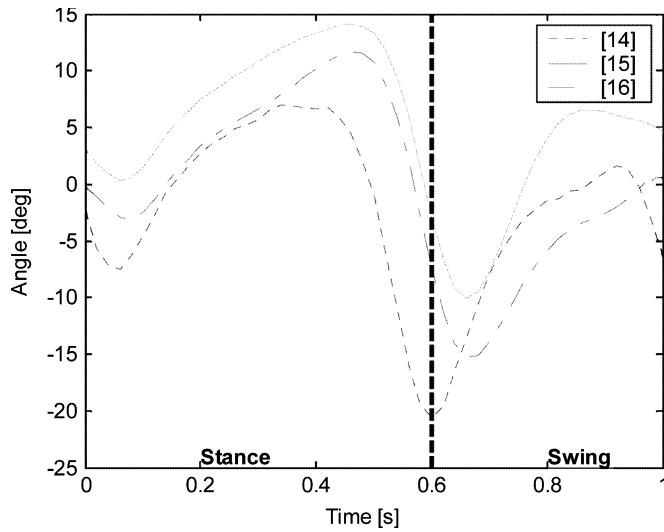
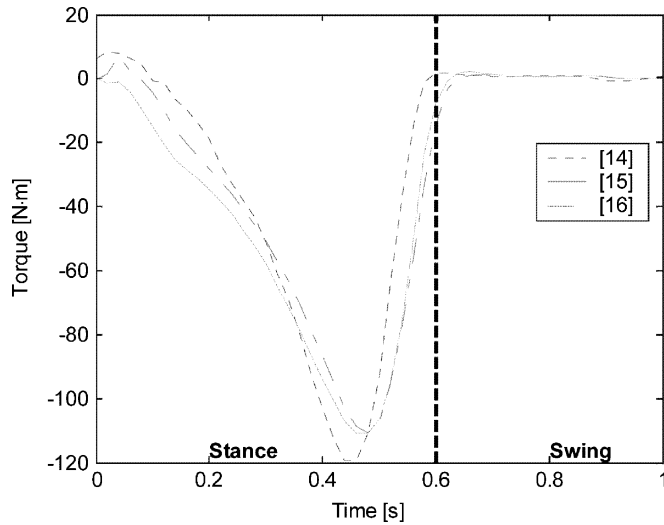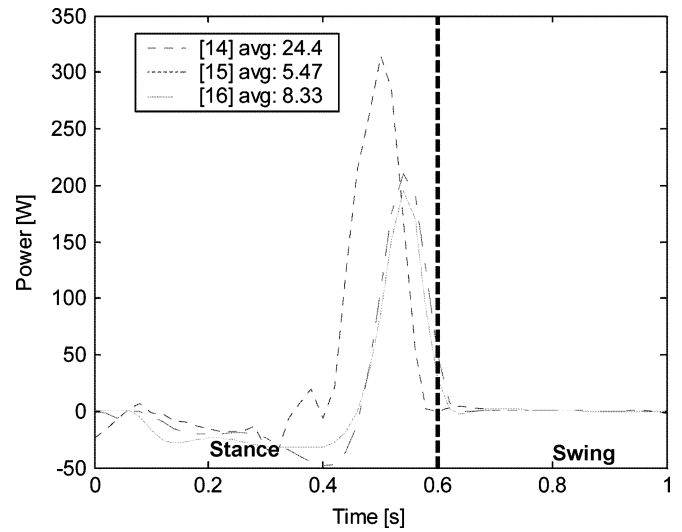Fig. 6.   Adjusted CGA data of the ankle flexion/extension angle.

Fig. 8.   Adjusted CGA data of the ankle flexion/extension instantaneous mechanical power. The average ankle power is positive, indicating the ankle does positive work and requires actuation.
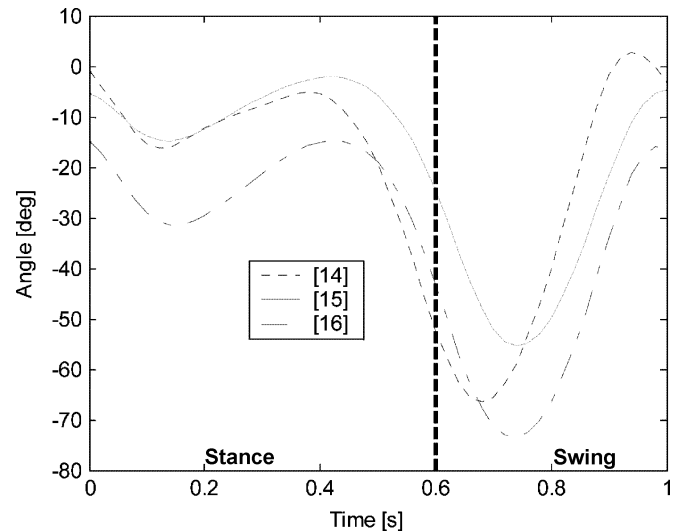

Fig. 7.   Adjusted CGA data of the ankle flexion/extension torque. Peak negative torque is very large (-120 N·m) and occurs in late stance phase. The ankle torque during swing is quite small.

Fig. 9.   Adjusted CGA data of the knee flexion/extension angle. The minimum angle is $-60°$, occurring in early-mid swing phase to enable the foot to clear the ground.

Conversely, if symmetric bidirectional actuators are considered, spring-loading would allow the use of low torque producing actuators. Although the ankle torque is large during stance, it is negligible during swing.

The instantaneous ankle mechanical power (shown in Fig. 8) is calculated by multiplying the joint angular velocity (derived from Fig. 6) and the instantaneous joint torque (Fig. 7). The ankle absorbs energy during the first half of the stance phase and releases energy just before toe-off. The average ankle power is positive, indicating that power production is required at the ankle.

C. Knee

The knee angle in Fig. 9 is characterized by knee flexion to create a horizontal hip trajectory. The knee buckles momentarily in early stance to absorb the impact of heel strike then undergoes a large flexion during swing. This knee flexion decreases the effective leg length, allowing the foot to clear the ground when swinging forward.

The CGA-based knee actuation torque is shown in Fig. 10. The required knee torque has both positive and negative components, indicating the need for a bidirectional actuator. The highest peak torque is extension in early stance (~60 N·m); hence, asymmetric actuators should be biased to provide greater extension torque.

Fig. 11 shows the CGA knee power. Since the average power is negative, many prosthetic devices use power dissipative devices (i.e., dampers) to mimic knee dynamics. However, the knee requires a large amount of positive power whenever the human is walking up an incline, or climbing stairs, so the BLEEX knee joint is actuated [17].
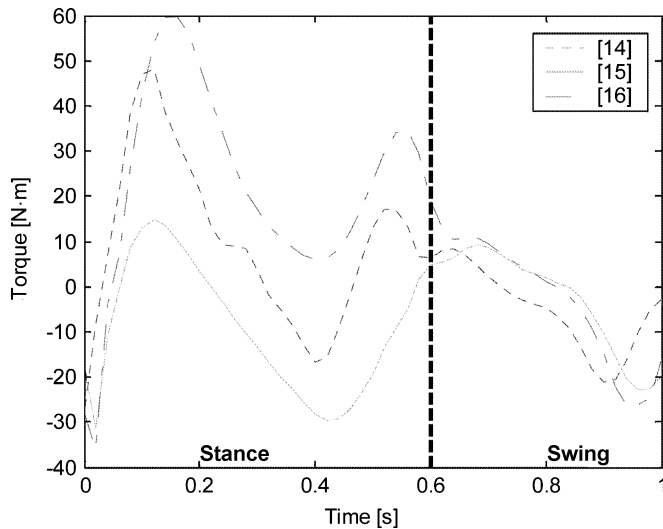
Fig. 10. Adjusted CGA data of the knee flexion/extension torque. An initial -35 N·m flexion torque is required at heel strike, followed by large extension torques ($\sim$60 N·m) to keep knee from buckling in stance phase.

Fig. 11. Adjusted CGA data of the knee flexion/extension instantaneous mechanical power. The negative average indicates power dissipation.
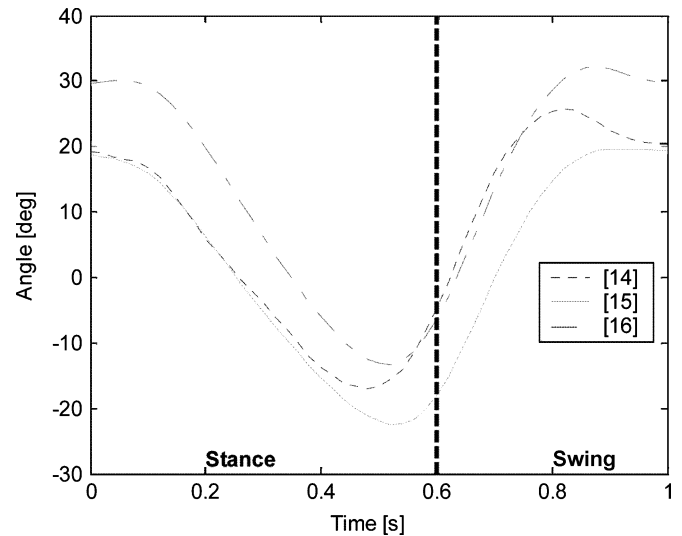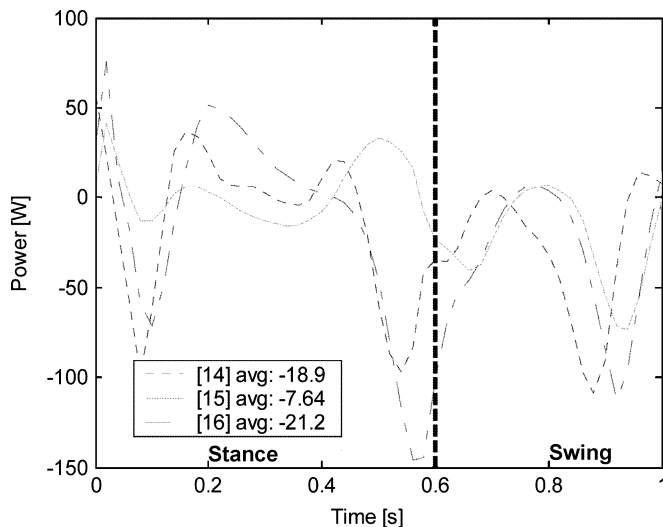

Fig. 12. Adjusted CGA data of the hip flexion/extension angle. The hip has an approximately sinusoidal behavior.
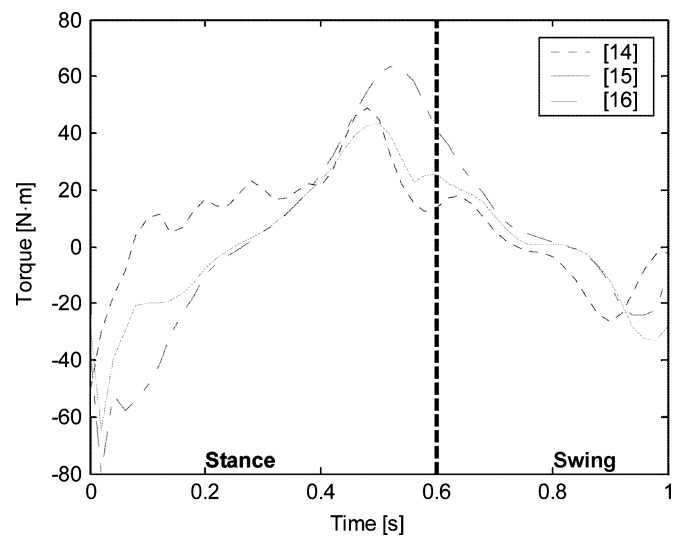

Fig. 13. Adjusted CGA data of the hip flexion/extension torque. The hip torque is bidirectional.

D. Hip

Fig. 12 details the hip angle while walking. The thigh moves in a sinusoidal pattern with the thigh flexed upward at heel strike to allow foot–ground contact in front of the person. This is followed by an extension of the hip through most of stance phase and a flexion through swing.

The hip torque in Fig. 13 is relatively symmetric (-80 to $+60$ N·m); hence, a bidirectional hip actuator is required. Negative extension torque is required in early stance as the hip supports the load on the stance leg. Hip torque is positive in late stance and early swing as the hip propels the leg forward during swing. In late swing, the torque goes negative as the hip decelerates the leg prior to heel strike.

Fig. 14 shows the instantaneous hip mechanical power. The hip absorbs energy during stance phase and injects it during toe-

off to propel the torso forward. The average power is positive, implying the need for active actuation.

Besides the flexion/extension joints at the ankle, knee, and hip, the other DOF in the human leg require substantially less mechanical power while walking [18]. Therefore, only the three flexion/extension joints were initially actuated on BLEEX. Later, actuation was added to the hip abduction/adduction joint to improve lateral balance. CGA data shows that the hip abduction/adduction joint requires the most power for nonflexion/extension joints [18].

VI. RANGE OF MOTION

The BLEEX kinematics are close to human leg kinematics, and therefore, the BLEEX joint ranges of motion are determined by examining human joint ranges of motion. At the very least,
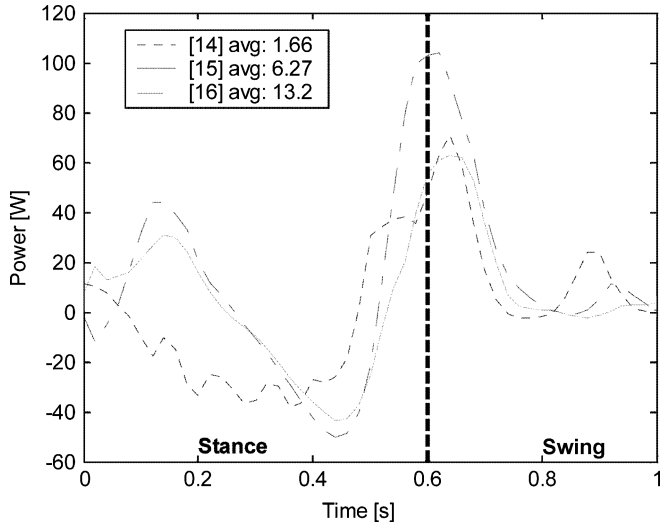
Fig. 14. Adjusted CGA data of the hip flexion/extension instantaneous mechanical power. The average hip power is positive, indicating an actuator is required at the hip.

Fig. 15. Triangular configuration of a linear actuator about a rotary joint. The moment arm R is perpendicular to the actuator and varies with joint angle θ.

TABLE II
BLEEX JOINT RANGES OF MOTION

	Human walking maximum	BLEEX maximum	Average military male maximum
Ankle flexion	14.1°	45°	35°
Ankle extension	20.6°	45°	38°
Ankle abduction	not available	20°	23°
Ankle adduction	not available	20°	24°
Knee flexion	73.5°	121°	159°
Hip flexion	32.2°	121°	125°
Hip extension	22.5°	10°	not available
Hip abduction	7.9°	16°	53°
Hip adduction	6.4°	16°	31°
Total rotation external	13.2°	35°	73°
Total rotation internal	1.6°	35°	66°

the BLEEX joint range of motion should be equal to the human range of motion during walking (see Table II), which can be found by examining CGA data [14]–[16]. Safety dictates that the BLEEX range of motion should not be more than the operator's range of motion (see Table II) [19]. For each DOF, Table II also lists the BLEEX range of motion which is, in general, larger than the human range of motion during walking and less than the maximum range of human motion.

The most maneuverable exoskeleton should ideally have ranges of motion slightly less than the human's maximum range of motion. However, BLEEX uses linear actuators (see Section VII) and so some of the joint ranges of motion are reduced to prevent the actuators' axes of motion from passing through the joint center. If this had not been prevented, the joint could reach a configuration where the actuator would be unable to produce a torque about its joint. Additionally, all the joint ranges of motion were tested and revised during prototype testing. For example, mock-up testing determined that the BLEEX ankle flexion/extension range of motion needs to be greater than the human ankle range of motion to accommodate the human foot's smaller DOF not modeled in the BLEEX foot.
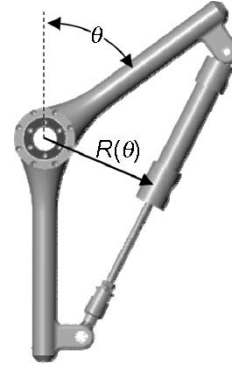
VII. ACTUATOR SELECTION AND SIZING

Hydraulic actuators have high specific power (ratio of actuator power to actuator weight), and thus are the smallest actuation option available. Also, hydraulic fluid is generally incompressible, leading to a relatively high-control bandwidth. BLEEX uses double-acting linear hydraulic actuators because of their compact size, low weight, and high-force capabilities. Rotary hydraulic actuators were not selected because they usually have either internal leakage or considerable friction.

In order to analytically determine the appropriate size of actuators, an equation for the actuator's torque capabilities must be determined. The maximum static pushing and pulling forces that a linear hydraulic actuator cylinder can supply is its cross-sectional area multiplied by the supply pressure (P_S). When a linear actuator is used to produce a torque about a rotary joint, its moment arm R changes as a function of the joint angle θ (Fig. 15). The torque the actuator can produce is its peak force times that moment arm

$$T_{\max\,\mathrm{push}} = P_S \frac{\pi D_{\mathrm{bore}}^2}{4} R(\theta) \qquad (1)$$

$$T_{\max\,\mathrm{pull}} = P_S \frac{\pi \left(D_{\mathrm{bore}}^2 - D_{\mathrm{rod}}^2\right)}{4} R(\theta) \qquad (2)$$

where D_{bore} is the actuator bore diameter and D_{rod} is the actuator rod diameter.

The problem of actuation design is to find a combination of actuator cross section, actuator endpoints, and supply pressure that provides the necessary torque but minimizes the hydraulic consumption. Since the BLEEX dynamics are close to human leg dynamics, the actuators must produce torque greater than the CGA data in order to walk. Additionally, the actuator must reach the desired ranges of motion while always being able to produce a minimum nominal torque. In general, there is not a unique solution, but many feasible possibilities.

To find a feasible actuator configuration, an actuator size (cross section, minimum length, and stroke), supply pressure, and one of the end-point positions were chosen for each joint. Assuming that the longest and shortest actuator lengths occur at the extremes of the joint's range of motion, the second end-point position of the actuator can be calculated (Fig. 16). The available actuator torque [(1) and (2)] can then be compared with the
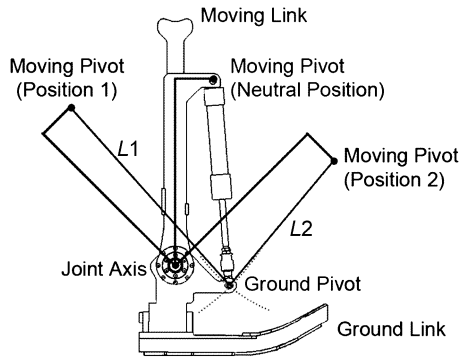
Fig. 16. Solving for the actuator end-point. First, an actuator and moving pivot location (in the neutral position) were chosen. The actuator is fully extended (length $L1$) and fully contracted (length $L2$) at the limits of motion (positions 1 and 2). The second end-point, the ground pivot, is found by the intersection of arcs of radii $L1$ and $L2$ centered at the moving pivot positions 1 and 2.
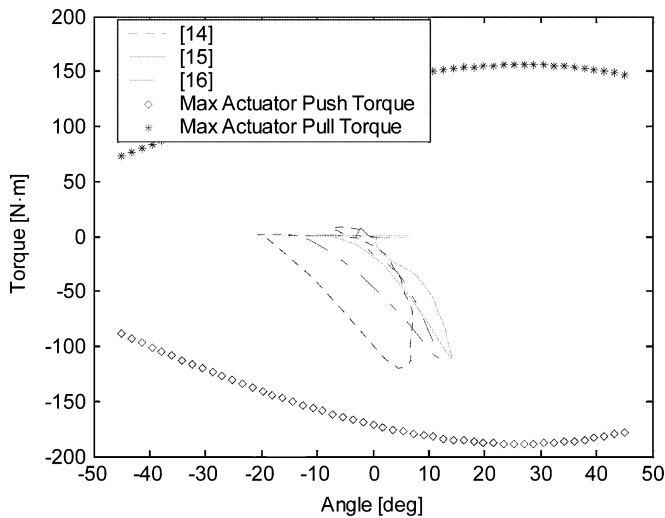

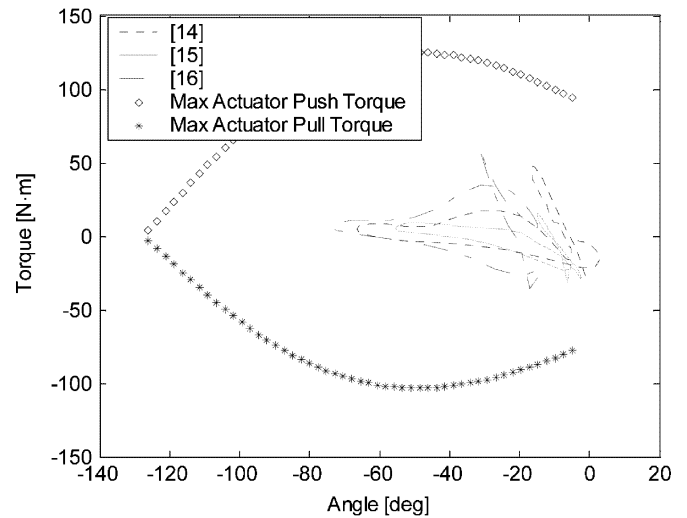Fig. 17. Ankle torque versus angle for CGA data and the max actuator torque.

Fig. 18. Knee torque versus angle for CGA data and the max actuator torque.

Fig. 19. Hip torque versus angle for CGA data and the max actuator torque.

required torques (as determined from CGA data). This process was iterated for each joint with different actuator sizes, mounting points, or supply pressures until a solution with enough torque and sufficiently low-power consumption was found.

Figs. 17–19 show the maximum torque versus angle plots [from (1) and (2)] for the BLEEX actuation compared to CGA data for the ankle, knee, and hip. BLEEX utilizes the smallest commercially available actuators (about 2-cm bore) along with a relatively low supply pressure of 6.9 MPa.

VIII. POWER ANALYSIS

Once the actuators were selected, the required hydraulic power for BLEEX to walk was estimated. Adding the absolute value of the ankle, knee, and hip flow rates for both the right and left legs yields the required system flow rate. Multiplying the system flow rate by the supply pressure (6.9 MPa) results in the total predicted hydraulic power consumption for BLEEX to walk, see Fig. 20.

The average hydraulic power consumption for BLEEX to walk is 1143 W, compared with 165 W of mechanical power consumed by a human during walking, according to CGA data [17].
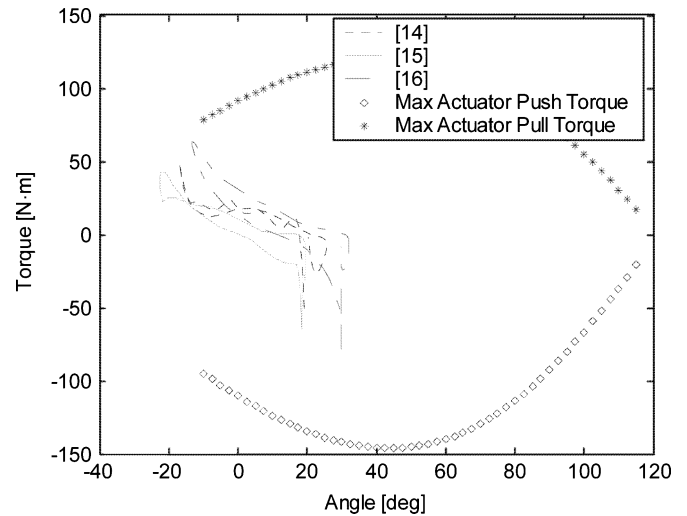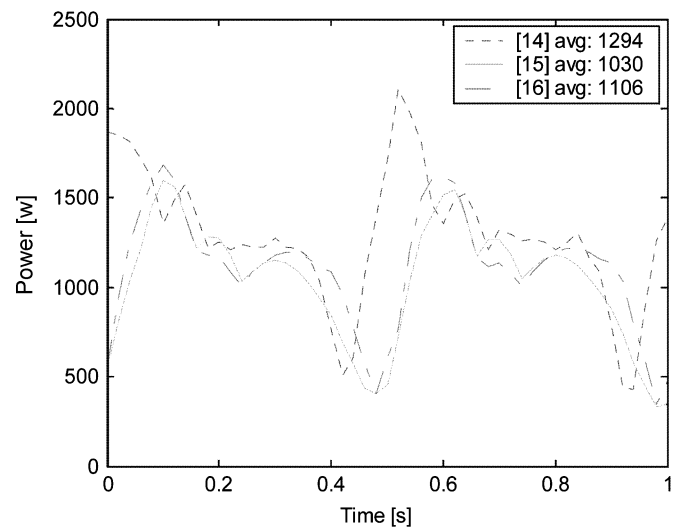

Fig. 20. Hydraulic power requirement for BLEEX walking.
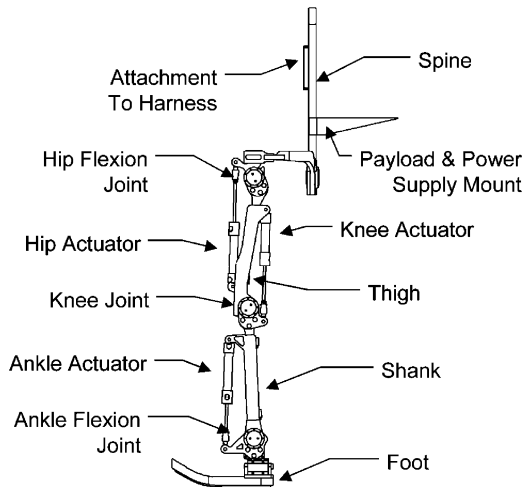
Fig. 21.   BLEEX Model (simplified to emphasize major components).

Fig. 22.   BLEEX foot design (exploded view).

Fig. 23.   BLEEX shank design.

The 14% efficiency of the hydraulic actuation is due to the pressure drop across the servo valves when the actuators require less pressure than the supply pressure. Even though it is a fairly low efficiency, this is standard for variable hydraulic systems and when comparing mechanical systems to their biological counterparts. A custom portable fuel-based and a monopropellant-based power source to power BLEEX are described in [20]–[22].

IX. BLEEX DESIGN

Fig. 21 is an overall model of BLEEX (simplified to emphasize the major components). The following sections discuss the critical features of the major components.

A. Foot Design

The BLEEX foot is a critical component due to its variety of functions:

a) It measures the location of the foot's center of pressure, and therefore, identifies the foot's configuration on the ground. This information is necessary for BLEEX control [12].

b) It measures the human's load distribution (how much of the human's weight is on each leg), which is also used in BLEEX control.

c) It transfers BLEEX's weight to the ground and so it must have structural integrity and exhibits long life in the presence of periodic environmental forces.

d) It is one of two places where the human and exoskeleton are rigidly connected and therefore it must be comfortable for the operator.

As shown in Fig. 22, the main structure of the foot has a stiff heel to transfer the load to the ground and a flexible toe for comfort. The operator's boot rigidly attaches to the top of the exoskeleton foot via a quick release binding. Along the bottom of the foot, switches detect which parts of the foot are in contact with the ground. For ruggedness, these switches are molded into a custom rubber sole. Also illustrated in Fig. 22 is the load-distribution sensor—a rubber "pressure tube" filled with
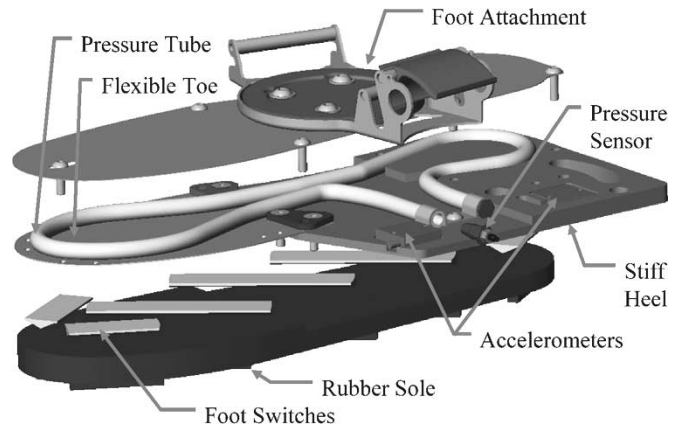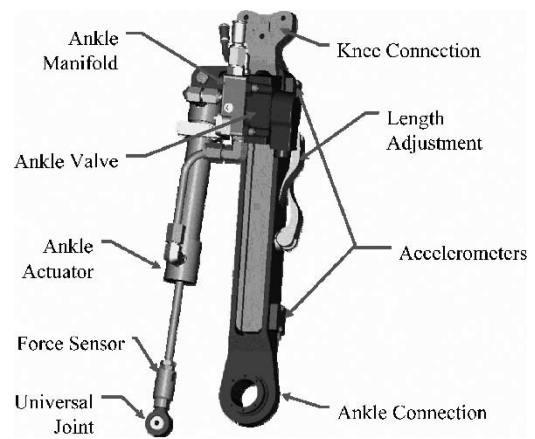
hydraulic oil and sandwiched between the human's foot and the main exoskeleton foot structure. Only the weight of the human (and not the exoskeleton) is transferred onto the pressure tube and measured by the sensor. This sensor is used by the control algorithm to detect how much weight the human places on their left leg versus their right leg.

B. Shank and Thigh Design

The main function of the BLEEX shank and thigh are to provide structural support and to connect the flexion/extension joints together (Figs. 23 and 24). Both the shank and thigh are designed to adjust to fit 90% of the population; they consist of two pieces that slide within each other and then lock at the desired length.

To minimize the hydraulic routing, manifolds were designed to route the fluid between the valves, actuators, supply, and return lines. These manifolds mount directly to the cylinders to reduce the hydraulic distance between the valves and actuator, maximizing the actuator's performance. The actuator, manifold, and valve for the ankle mount to the shank, while the actuators, manifold, and valves for the knee and hip are on the thigh. One manifold, mounted on the knee actuator, routes the hydraulic fluid for the knee and hip actuators.
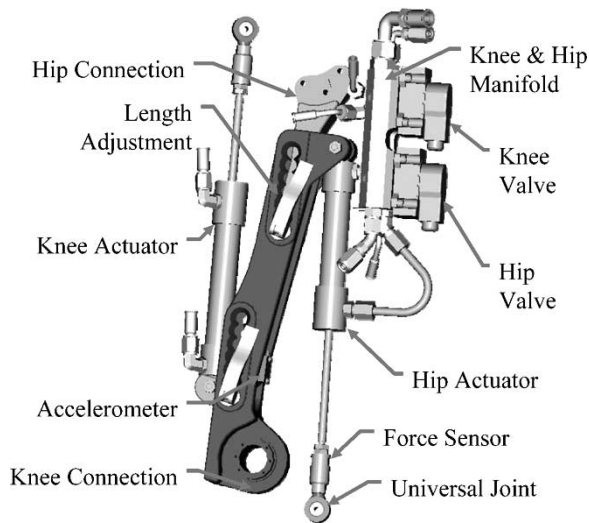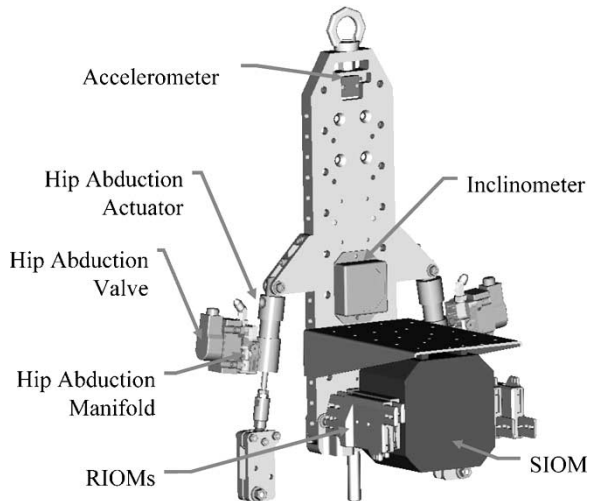
Fig. 24.   BLEEX thigh design.

Fig. 25.   BLEEX torso design (back view).

C. Torso Design

As shown in Fig. 25, the BLEEX torso connects to the hip structure (shown in Fig. 2). The power supply, controlling computer, and payload mount to the rear side of the torso. An inclinometer mounted to the torso gives the absolute angle reference for the control algorithm. A custom harness mounts to the front of the torso to hold the exoskeleton to the operator. Besides the feet, the harness is the only other location where the user and exoskeleton are rigidly connected. Fig. 25 also illustrates the actuator, valve, and manifold for the hip abduction/adduction joint.

Custom electronic boards (RIOMs) are used to acquire all of the sensor data and communicate with the control computer (called the supervisor I/O module or SIOM) [13]. Some of the RIOMs along with the SIOMs are attached to the BLEEX torso, see Fig. 25. The other RIOMs are attached to the shanks and thighs, but were omitted from the figures for clarity.

Fig. 26.   Final BLEEX design.

D. Final Design

Fig. 26 shows the current BLEEX design. The black backpack encloses the power source, controller computer, and payload.

X. EXPERIMENTALLY MEASURED PERFORMANCE

The exoskeleton actuation was designed using human CGA data, which assumes that the BLEEX kinematics and dynamics closely match human leg kinematics and dynamics. To verify this assumption, and for use in future exoskeleton development, torque and angle data was measured from BLEEX walking. The measured data for the ankle, knee, and hip flexion/extension joints are shown in Figs. 27–29. The figures show both the torque desired by the controller and the torque actually measured from the sensors. Additionally, the plots show the actuator limit curves and so the measured data can be easily compared with the CGA curves (Figs. 17–19).

All of the measured torque curves lie within the maximum actuator curves, which shows BLEEX has sufficient torque to walk without saturating the actuators. However, a quick comparison of the measured torque vs. angle curves (Figs. 27–29) and CGA torque vs. angle curves (Figs. 17–19) reveals that there are some distinct differences. Following are some of the more significant causes for these discrepancies:

a) The BLEEX knee is always bent by at least 5° allowing the leg to always exert a vertical force. This offsets the ankle and hip angles slightly positive and the knee angle slightly negative. The bent knee also shifts the required knee torques more positive than a straight knee.
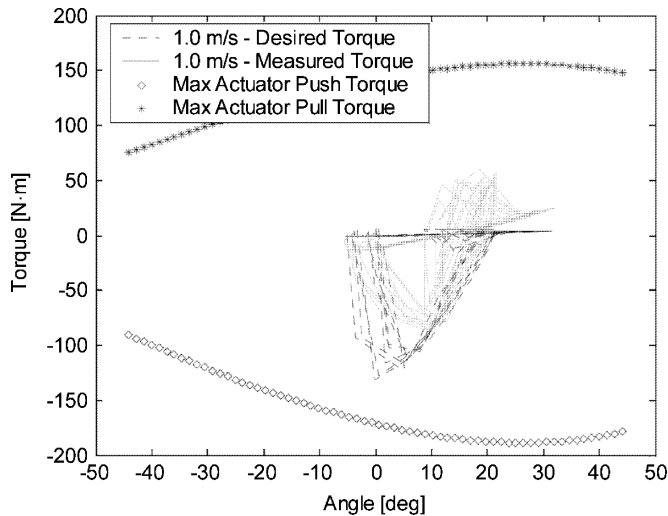
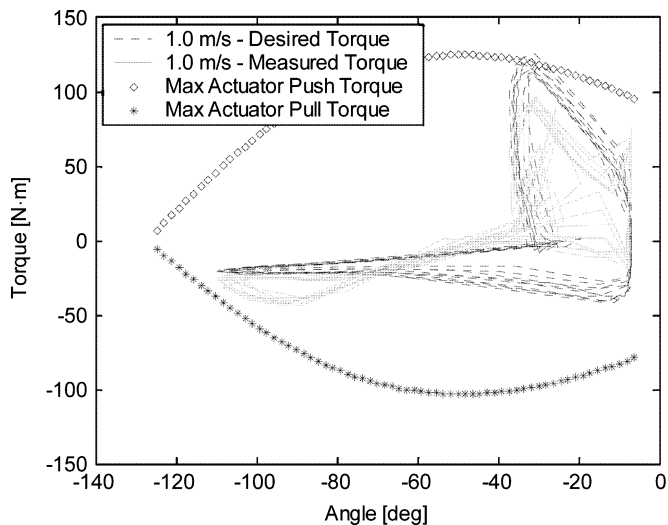Fig. 27.   Ankle torque versus angle data measured from BLEEX walking.

Fig. 28.   Knee torque versus angle data measured from BLEEX walking.
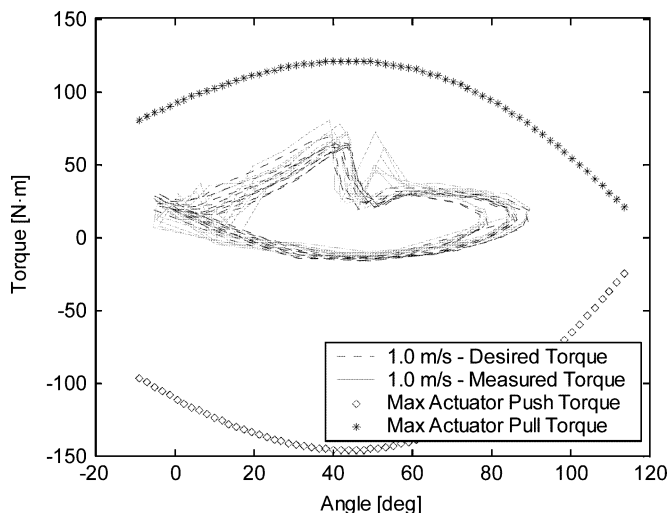

Fig. 29.   Hip torque versus angle data measured from BLEEX walking.

b) While the BLEEX torso weighs close to a human torso, its center of gravity is behind the human torso's center of gravity. This creates a negative shift of the ankle and hip torques and a positive shift in the knee torque.

c) The local torque control on each joint actuator is not perfected and so the desired torques are not always achieved.

Generally, measured data from the knee and hip joints differ the most from the CGA data used to design the actuation. Both the knee and hip also consume more energy per step (area encircled by a torque/angle curve) than predicted, but the ankle consumes less energy.

XI. CONCLUSION AND FUTURE WORK

Approximating the BLEEX kinematics and dynamics as the same as human leg kinematics and dynamics allowed the BLEEX actuation to be designed based on CGA data. This resulted in a BLEEX leg with 7 DOF and four of them are actuated (flexion/extension at the ankle, knee, and hip and abduction/adduction at the hip). The actuator sizes, actuator mounting points, and servo valves were also selected using CGA data. Initial calculations indicated that BLEEX should consume about 1140 W of power while walking. The measured torque vs. angle curves from BLEEX demonstrate that the CGA-based design yielded an exoskeleton with sufficient torque to walk. However, the measured curves do differ from the CGA curves, showing that the BLEEX kinematics and dynamics do not fully match the human; therefore, further design improvement can be accomplished based around the more accurate measured torque vs. angle curves.

While there is still significant work remaining, BLEEX has successfully walked while carrying its own weight and producing its own power. This makes BLEEX the first energetically autonomous lower extremity exoskeleton capable of carrying a payload. Currently, BLEEX has been demonstrated to support up to 75 kg, walk at speeds up to 1.3 m/s, and shadow the operator through numerous maneuvers without any human sensing or preprogrammed motions.

Current work on BLEEX includes continued analysis of the measured performance data in order to improve the actuation design and efficiency. Considerable work is also being performed to decrease the overall power consumption of BLEEX, either by reduced actuation, additional passive elements, or improved efficiency. Efforts to reduce the weight and size of the exoskeleton structure are critical to improve the system efficiency, increase payload capacity, and lead to a slimmer more fieldable design. Hopefully with continued improvement to the system's fieldability, the BLEEX will become a practical method of increasing human-carrying capacity and endurance through rough environments.

REFERENCES

[1] B. J. Makinson, Research and development prototype for machine augmentation of human strength endurance, Hardiman I project, General Electric Co., Schenectady, NY, 1971. Tech. Rep. S-71-1056.
[2] M. Vukobratovic, D. Hristic, and Z. Stojiljkovic, "Development of active anthropomorphic exoskeletons," *Med. Biol. Eng.*, vol. 12, no. 1, pp. 66–80, Jan. 1974.

[3] H. Kawamoto and Y. Sankai, "Power assist system HAL-3 for gait disorder person," *Lecture Notes Computer Science, vol 2398: Proc. 8th Int. Conf. Computers Helping People with Special Needs*, Berlin, Germany: Springer-Verlag, 2002.

[4] K. Yamamoto, K. Hyodo, M. Ishii, and T. Matsuo, "Development of power assisting suit for assisting nurse labor," *JSME Int. J. Series C.*, vol. 45, no. 3, pp. 703–711, Sep. 2002.

[5] Y. Mori, K. Takayama, and T. Nakamura, "Development of straight style transfer equipment for lower limbs disabled," in *Proc. IEEE ICRA*, New Orleans, LA, vol. 3, May 2004, pp. 2486–2491.

[6] D. Johnson, D. Repperger, and G. Thompson, "Development of a mobility assist for the paralyzed, amputee, and spastic patient," in *Proc. 15th Southern Biomedical Eng. Conf.*, Dayton, OH, Mar. 29–31, 1996, pp. 67–70.

[7] J. Misuraca and C. Mavroidis, "Lower limb human muscle enhancer," in *Proc. Symp. Advances in Robot Dynamics and Control, ASME Int. Mechanical Engineering Congr. Exposition*, New York, Nov. 2001.

[8] J. Pratt, B. Krupp, C. Morse, and S. Collins, "The RoboKnee: An exoskeleton for enhancing strength and endurance during walking," in *Proc. IEEE ICRA*, New Orleans, LA, vol. 3, May 2004, pp. 2430–2435.

[9] C. Fleischer, C. Reinicke, and G. Hommel, "Predicting the intended motion with EMG-signals for an exoskeleton orthosis controller," in *Proc. IEEE Int. Conf. Intelligent Robots and Systems*, Edmonton, Canada, Aug. 2005, pp. 2029–2034.

[10] K. Naruse, S. Kawai, H. Yokoi, and Y. Kakazu, "Design of compact and lightweight wearable power assist device," presented at the *ASME Int. Mechanical Eng. Congr. and Exposition*, Washington, DC, Nov. 2003.

[11] D. Ferris, J. Czerniecki, and B. Hannaford, "An ankle-foot orthosis powered by artificial muscles," presented at the *25th Meeting of the American Society of Biomechanics*, San Diego, CA, Aug. 2001.

[12] H. Kazerooni, L. Huang, and R. Steger, "On the Control of the Berkeley lower extremity exoskeleton (BLEEX)," in *IEEE ICRA*, Barcelona, Spain, Apr. 18–22, 2005, pp. 4353–4360.

[13] S. Kim, G. Anwar, and H. Kazerooni, "High-speed communication network for controls with application on the exoskeleton," presented at the *American Control Conf.*, Boston, MA, Jun. 2004.

[14] A. Winter, Gait Data. Int. Soc. Biomechanics, Biomechanical Data Resources. [Online]. Available: http://guardian.curtin.edu.au/org/data/

[15] C. Kirtley, CGA Normative Gait Database, Hong Kong Polytechnic Univ. [Onine]. Available: http://guardian.curtin.edu.au/cga/data/

[16] J. Linskell, CGA Normative Gait Database, Limb Fitting Centre, Dundee, Scotland. [Onine]. Available: http://guardian.curtin.edu.au/cga/data/

[17] A. Chu, H. Kazerooni, and A. Zoss, "On the biomimetic design of the Berkeley lower extremity exoskeleton (BLEEX)," in *Proc. IEEE ICRA*, Barcelona, Spain, Apr. 18–22, 2005, pp. 4345–4352.

[18] J. Rose and J. G. Gamble, *Human Walking*, 2nd ed. Baltimore: Williams & Wilkins, 1994.

[19] W. Woodson, B. Tillman, and P. Tillman, *Human Factors Design Handbook*. New York: McGraw-Hill, pp. 550–552, 1992.

[20] K. Amundson, J. Raade, N. Harding, and H. Kazerooni, "Hybrid hydraulic-electric power unit for field and service robots," in *Proc. IEEE Int. Conf. Intelligent Robots Syst.*, Edmonton, Canada, Aug. 2–6, 2005, pp. 3453–3458.

[21] T. McGee, J. Raade, and H. Kazerooni, "Monopropellant-driven free piston hydraulic pump for mobile robotic systems," *J. Dyn. Syst., Meas. Control*, vol. 126, pp. 75–81, Mar. 2004.

[22] J. Raade and H. Kazerooni, "Analysis and design of a novel power source for mobile robots," *IEEE Trans. Autom. Sci. Eng.*, vol. 2, no. 3, pp. 226–232, Jul. 2005.

Adam B. Zoss received the B.S. degree from the University of Texas, Austin, in 2000 and the M.S. degree from the University of California, Berkeley, in 2003, both in mechanical engineering. He is currently working toward the Ph.D. degree in the Robotics and Human Engineering Laboratory, University of California, researching robotics and mechatronics.

H. Kazerooni (S'84–M'85) received the M.S. and Ph.D. degrees from the Massachusetts Institute of Technology, Cambridge, in 1982 and 1985, respectively, both in mechanical engineering.

He is currently a Professor in the Mechanical Engineering Department, University of California, Berkeley, and the Director of the Berkeley Robotics and Human Engineering Laboratory.

Andrew Chu received the B.S., M.S., and Ph.D. degrees from the University of California, Berkeley, in 2000, 2002, and 2005, respectively, all in mechanical engineering.

He is currently a Research Scientist, Siemens, Concord, CA.